



# Neuromuscular control of reactive behaviors for undulatory robots

M. Sfakiotakis, D.P. Tsakiris\*

*Institute of Computer Science-FORTH, Vassilika Vouton, P.O. Box 1385, GR-71110 Heraklion, Greece*

## Abstract

Undulatory locomotion is studied as a biological paradigm of versatile body morphology and effective motion control, adaptable to a large variety of unstructured and tortuous environmental conditions. Computational models of undulatory locomotion have been developed, and validated on a series of robotic prototypes propelling themselves on sand. The present paper explores in simulation neuromuscular motion control for these undulatory robot models, based on biomimetic central pattern generators and on information from distributed distance sensors. This leads to reactive control schemes, which achieve (i) traversal of corridor-like environments, and (ii) formation control for swarms of undulatory robots.

© 2006 Elsevier B.V. All rights reserved.

*Keywords:* Neural control; Central pattern generators; Biomimetic robotics; Undulatory locomotion; Sensors; Closed-loop control; Polychaete annelids

## 1. Introduction

Motion control is one of the most significant problems for emerging robotic applications dealing with locomotion in unstructured environments, which range from endoscopy to planetary exploration [4,13,31,34]. Drawing inspiration from biology, where this problem has been effectively addressed by the evolutionary process, can help the design of agile robots able to adapt robustly to a variety of environmental conditions. Such an intriguing biological paradigm is offered by the polychaete annelid worms, whose locomotion is characterized by the combination of a unique form of tail-to-head body undulations, with the rowing-like action of numerous lateral appendages, called parapodia, distributed along their segmented body [6,11]. This provides the worms with distinctive locomotory modes, increasing their swimming, terrain traversing and burrowing capabilities over water, sand, mud and sediment. These locomotory modes have been modeled computationally and validated via robotic prototypes propelling themselves on sand [30,31,34].

Undulatory locomotion in annelids and other organisms, as well as in robots, is achieved through appropriate

coupling of internal shape changes (typically a traveling body wave) to external motion constrains (typically frictional forces from the interaction with the locomotion environment). Evidence exists [21,9,27] that motion control of the annelid undulatory locomotion is based on central pattern generators (CPGs), which are neuronal circuits able to produce rhythmic motor patterns in an organism, even in the absence of sensory input or of input from higher cognitive elements; such inputs may modulate the rhythmic activity of the CPG [23,2]. The typical morphology of annelids [11,6,27] hints at a sequential, modular and distributed sensing and control architecture, not unlike that of the CPG controlling the undulatory swimming of lamprey eels, which has been extensively studied in neurobiology [27,12] and modeled at various levels of detail [10,12,14,24,18,19,28]. From an engineering viewpoint, interest in CPG-based locomotion controllers, especially for undulatory mechanisms, stems not only from their elegance, but also from their potential to lead to distributed, fault-tolerant and robust motion control architectures [4,30,26,33,7,22,15,16].

The literature on undulatory robotic systems has mainly focused on mechanical design and open-loop control (gait generation). However, in order for such devices to be able to operate in the complex environments for which they are intended, they require exteroceptive sensing to close the

\*Corresponding author. Tel.: +30 2810 391708; fax: +30 2810 391601.  
E-mail address: [tsakiris@ics.forth.gr](mailto:tsakiris@ics.forth.gr) (D.P. Tsakiris).

loop and implement more complex behaviors, either for single robots (e.g., obstacle avoidance, pursuit of moving targets) or for multi-robot swarms (e.g., formation control, cooperative exploration) [32]. This paper presents computational models of CPG-based neuromuscular control for undulatory robotic systems in Section 2, and explores in simulation the use of sensory information from distributed sensors for the generation of reactive behaviors (centering and body wave shaping in corridor environments) in Section 3. This modulation of the CPG dynamics by sensory information appears not to destroy rhythmogenesis, although it may alter its characteristics.

Many potential applications for undulatory robots (e.g., site inspection, search-and-rescue missions, ocean sampling) involve tasks which could be more efficiently addressed by multiple robotic agents operating as a swarm. A significant body of work is available regarding swarms of conventional mobile robots and of underwater or aerial vehicles (see [32,17,29] and references therein); however, swarms of undulatory robots do not appear to have been investigated. Swarming behavior is important for biological organisms (e.g., for mutual protection, like the fish “bait-ball” rotating formations). This paper, then, also considers in Section 3 the extension of the developed neuromuscular control schemes to formation control problems for swarms of undulatory robots.

**2. Neuromuscular control for undulatory robots**

The main components involved in modeling an undulatory locomotor are: (i) the body mechanical model, (ii) the body shape control strategy and (iii) the force model of the body’s interaction with the environment. The implementation of these components in the present study is described next.

*2.1. Body mechanics*

Undulatory locomotors can be modeled as multi-link articulated robots comprising serially connected links, the equations of motion of which can be obtained from their Lagrangian dynamics [34]. A computational model of a planar undulatory mechanism has been developed, based on a serial kinematic chain of  $N$  identical rigid 2D links, with the center of mass for each link being at its middle (we

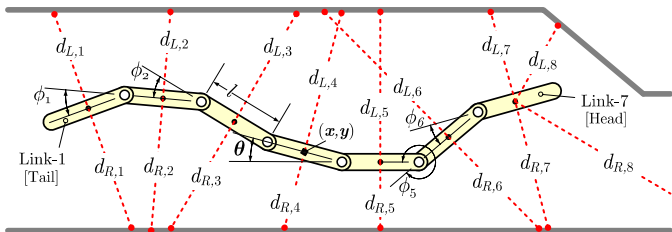


Fig. 1. Computational model of a seven-link undulatory mechanism and its sensor array (distance sensors).

consider  $N$  odd; the case of  $N = 7$  is shown in Fig. 1). The links are interconnected by planar revolute joints, which are independently actuated, via applied torques, to control the shape of the mechanism.

The position  $(x, y)$  and orientation  $\theta$  of the central link describe the global pose of the mechanism with respect to an inertial coordinate frame on the plane, and can be represented by an element  $g$  of the group  $G = SE(2)$ , the Special Euclidean group of order 2. The Lie algebra element, corresponding to  $g$ , is  $\zeta \triangleq g^{-1}\dot{g} \in \mathcal{G} = se(2)$  and describes the *body velocity* of the central link. The joint angle vector  $r = (\phi_1, \dots, \phi_{N-1})$  describes the system’s body shape.

The Euler–Lagrange equations of motion can be *reduced* [34,5,20,8,25] by exploiting the invariance of the mechanism to changes in inertial position and orientation, expressed as *Lie group symmetries* exhibited by the system (for details see [34]):

$$\begin{aligned} \dot{g} &= g[-\mathbf{A}(r)\dot{r} + \mathbf{I}^{-1}(r)p], \\ \dot{p} &= ad_{\zeta}^* p + f_T + f_N, \\ \tilde{M}(r)\ddot{r} + \dot{r}^T \tilde{C}(r)\dot{r} + \tilde{N} &= B(r)\tau, \end{aligned} \tag{1}$$

where the matrices  $\mathbf{A}(r)$  and  $\mathbf{I}(r)$  are the local forms of the *mechanical connection* and the *locked inertia tensor*, respectively;  $p$  is the body momentum;  $f_T, f_N$  are the external frictional forces in the tangential and normal directions of the central link, which are obtained from the frictional force models described in Section 2.3. The first two equations in (1) describe the effect of body shape changes and of the interaction with the environment on the global pose of the mechanism. The third equation describes the evolution of the body shape, as a function of the control input, which is the joint torques  $\tau$ . In the present model, these torques are provided, for each joint, by a pair of antagonistic muscles, which are driven by the motoneuron outputs of the locomotor CPG described in Section 2.2. These computational models may be extended to polychaete-like mechanisms by the inclusion of parapodial links [31].

*2.2. CPG-based propulsive wave generation*

Neuromuscular body shape control schemes have been developed [33,30], based on connectionist models of the CPG which controls lamprey swimming (see, e.g., [10,14]), formed as a chain of (identical) segmental oscillators (S.O.s), properly interconnected to generate a wave of joint activation. Each S.O. comprises interneurons, which produce the rhythmic pattern, and motoneurons, which transmit the rhythmic pattern to the muscles activating a joint. Each of the S.O. neurons is modeled as a leaky integrator [2,14], where the mean membrane potential  $m_j$  of neuron  $j$  is

$$T_j \frac{dm_j}{dt} = -m_j + \sum_k q_{j,k} M_k + I_j, \tag{2}$$

where  $M_j = (1 + e^{-(m_j+b_j)})^{-1}$  is the neuron's output, namely its short-term average firing frequency, while  $b_j$  is the neuron's bias,  $T_j$  is its time constant,  $q_{j,k}$  is the synaptic weight of the connection from neuron  $k$  (providing input  $M_k$ ) to neuron  $j$ , and  $I_j$  is the applied external tonic input. The neurons of each S.O. are arranged in two symmetric sub-networks that create oscillations in antiphase through mutual inhibition; the specific architecture utilized and the corresponding neural signals are shown in Fig. 2. The torques applied to each body joint are determined by the outputs of the corresponding motoneurons, via the activation of a pair of antagonistic lateral muscles. Using the spring-and-damper muscle model described in [10], the torque  $\tau_i$  applied to the  $i$ th joint is obtained as

$$\tau_i = \alpha_i(M_{i,L} - M_{i,R}) + \beta_i(M_{i,L} + M_{i,R} + \gamma_i)\phi_i + \delta_i\dot{\phi}_i, \quad (3)$$

where the motoneuron output on the left and right sides of the corresponding S.O. is denoted by  $M_{i,L}$  and  $M_{i,R}$ , respectively;  $\phi_i$  is the joint angle (cf. Fig. 1); the  $\alpha_i, \beta_i, \gamma_i$  and  $\delta_i$  parameters of the muscle model are detailed in [10].

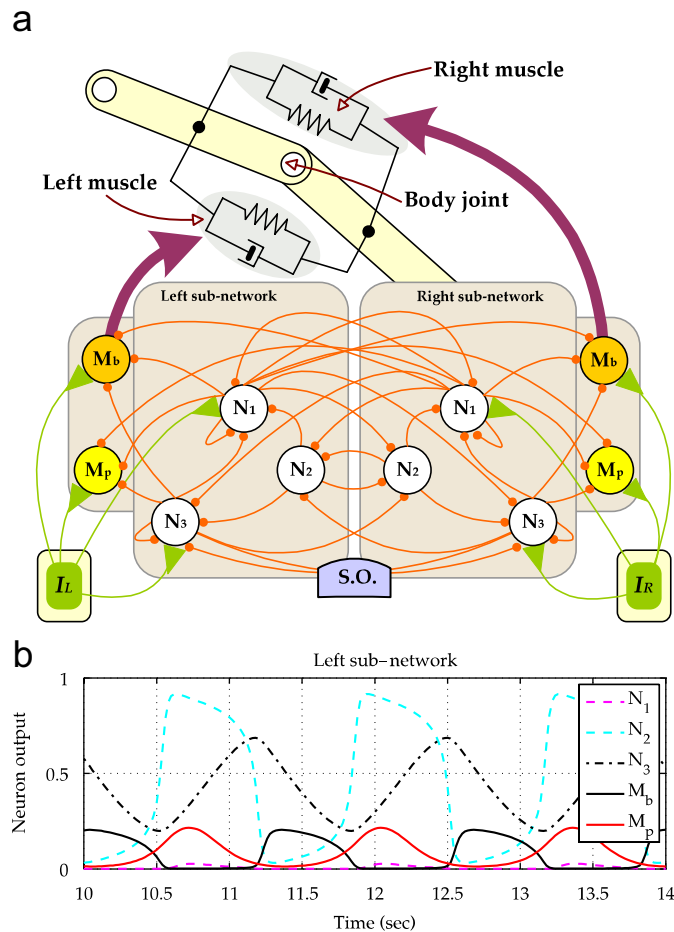


Fig. 2. Segmental oscillator architecture: (a) Schematic diagram (interneurons are denoted by N and motoneurons by M), showing the activation of the pair of antagonistic muscles actuating a body (resp., parapodial) joint through the output of the body motoneurons  $M_b$  (resp.,  $M_p$ ). (b) Neuron outputs of the left S.O. sub-network for  $I_L = I_R = 0.5$ .

The motoneuron output characteristics can be altered by tonic (i.e., nonoscillating) inputs to the left and right sub-networks of the segmental oscillators ( $I_L$  and  $I_R$ , respectively) [33].

Coupled to the body's mechanical model, the locomotor CPG yields motion in a straight line for  $I_L = I_R = I$ , where the tonic input level  $I$  alters the amplitude and/or frequency of the body wave via the motoneuron outputs; turning motions of the mechanism are instigated by unequal tonic inputs ( $I_L \neq I_R$ ) to the two sides of the CPG. These tonic inputs are modulated by sensory information to implement the reactive behaviors described in Section 3. The successful generation of these behaviors depends on the intersegmental connectivity of the CPG, which affects critically the response of motoneurons to variations of the tonic input [18,19,24,28,33].

### 2.3. Interaction with the environment

In order to model the interaction of the undulatory mechanism with its environment (either terrestrial or aquatic), various resistive friction models have been utilized, in which the force on an individual body link comprises decoupled components in the normal and tangential direction of motion, both of which depend on the links' velocity (for details see [34,30]). The sensor-based neural control schemes described here were shown in simulation to be able to generate various reactive behaviors in conjunction with any of these force models. For simplicity, the simulation studies presented here utilize a viscous friction model, in which the tangential and normal components of the force applied to the  $i$ th link are obtained as  $F_T^i = -c_T v_T^i$  and  $F_N^i = -c_N v_N^i$ , where  $v_T^i$  and  $v_N^i$  are the respective components of the velocity of the  $i$ th link.

The ratio  $c_N/c_T$  of the force coefficients is a key parameter in undulatory locomotion. For  $c_N > c_T$ , the overall locomotion direction is *opposite* to that of the wave direction; therefore, forward propulsion is achieved by a head-to-tail body wave. This type of undulatory locomotion (dubbed *eel-like* here) is by far the most common in nature, both on land and in the water, and has been replicated in the vast majority of existing undulatory robots (e.g., [4,13,7,16,22,8]). For  $c_N < c_T$ , the locomotion is *along* the direction of wave propagation; hence, forward motion is achieved by a tail-to-head wave. In nature, this locomotion mode is exhibited mainly by the polychaete annelid marine worms, but also by certain protozoa, flagellates and zoospores. Robotic prototypes implementing this novel type of undulatory locomotion (dubbed *polychaete-like* here) are described in [34,31].

### 3. Reactive behaviors for undulatory robots

The continuously changing shape of the elongated articulated body of undulatory robots complicates the generation of sensor-based reactive behaviors. Systematic guidelines for the selection of parameters like the number,

type and topology of sensors are currently lacking; however, the typical morphology of the corresponding biological organisms hints at a distributed sensing and control architecture [6,9,11,21,26,27]. We consider distance sensors placed on each robot link, which are employed to dynamically adjust the propulsive wave amplitude, while the head link may incorporate additional sensors (e.g., distance, vision), whose output is utilized in steering the mechanism.

In accordance with this approach, the simulation studies presented here are based on an undulatory mechanism composed of seven identical links, each equipped with a distance sensor pair aiming at  $\pm 90^\circ$  with respect to the link's main axis, while the head link features an additional distance sensor pair, aiming at  $\pm 45^\circ$  (Fig. 1). The locomotor CPG comprises 20 segmental oscillators, with the motoneuron outputs from (roughly) every third S.O. utilized to provide torque signals to the six joints of the mechanism, through the activation of antagonistic muscles.

The SIMUUN simulation environment for undulatory locomotion [30] was employed to model the above system and to implement the reactive behaviors described below, making use of the modules provided for emulating the distance sensors and for implementing 2D models of the world that the mechanism(s) operates in.

### 3.1. Reactive centering control

This reactive behavior is inspired by the centering response exhibited by bees when flying through narrow gaps, which has been attributed to their balancing the retinal motion perceived by each of their two wide field-of-view compound eyes. It was originally implemented on nonholonomic mobile robots, using panoramic optical flow information [3,1]. Adaptation to the more challenging dynamics of undulatory robotic locomotors relies on balancing the weighted sum of the distance sensor outputs to the left and right sides of the robot [32]. Assuming  $M$  pairs of distance sensors, and denoting by  $d_{L,i}$  and  $d_{R,i}$  ( $1 \leq i \leq M$ ) the outputs for such a sensing array, the control law to realize the undulatory centering behavior is, then, implemented via the tonic input signals applied to the left and right sides of the CPG:

$$I_L(t) = I - k_n s(t) \quad \text{and} \quad I_R(t) = I + k_n s(t) \quad \text{for } k_n > 0. \quad (4)$$

The distance balancing metric  $s(t)$  above is obtained as

$$s(t) = \frac{1}{\sum_{i=1}^M w_i d_{L,i}(t)} - \frac{1}{\sum_{i=1}^M w_i d_{R,i}(t)}, \quad (5)$$

where the weights  $w_i$  determine the relative contribution of the  $M$  sensor pairs.

A series of simulation studies performed demonstrates the ability of the integrated neural control scheme to successfully navigate the robot through various corridor-like courses, both for eel-like and for polychaete-like interaction with the environment, when utilizing sensory

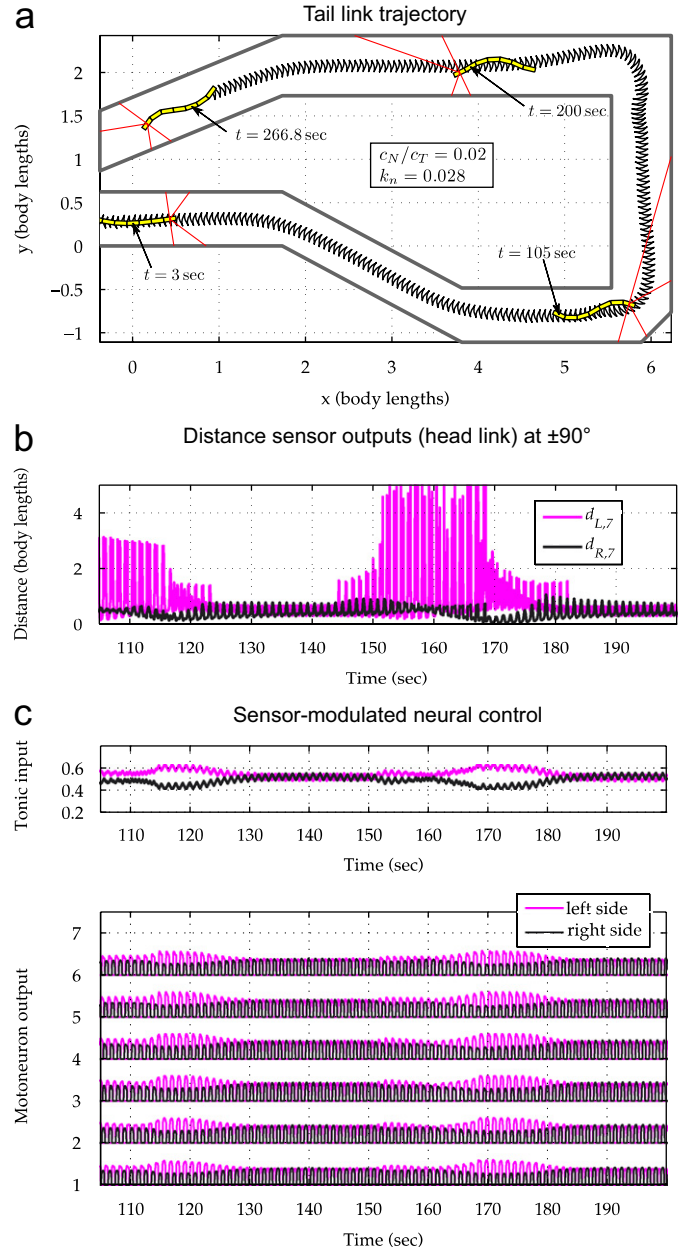


Fig. 3. Neural control of the undulatory centering behavior, for polychaete-like locomotion: (a) trajectory of the mechanism. For the interval  $t \in [105\text{ s}, 200\text{ s}]$ ; (b) measurements from a distance sensor pair, and (c) the corresponding tonic input signals and motoneuron outputs of the locomotor CPG.

information from the head link. Typical results are shown in Fig. 3. Equal, on the average, tonic inputs in the two sides of the CPG indicate straight-line movement along the center of the corridor (Fig. 3c). The oscillatory component in the tonic input is due to its modulation by the sensory data, which oscillate in response to the robot undulations. Removal of this component by temporal filtering of either the tonic input or of the sensory data yields a similar overall behavior, but diminishes the reactivity of the scheme and increases its computational cost; therefore, it

is not used here. It is noteworthy that the modulation of the CPG dynamics, via the tonic input, by such noisy and variable raw sensory data, does not appear to destroy the rhythogenesis of the CPG.

### 3.2. Reactive amplitude shaping

Reactive amplitude shaping refers to the use of information from sensors distributed along the undulatory mechanism to adjust the amplitude of the body wave, in order to enable the navigation of environments involving variable corridor widths and/or tighter turns, when used in conjunction with reactive centering. The approach adopted involves an adaptive gain  $r(t)$ , which is used to scale the tonic input signals:  $I_L(t) = r(t)(I - k_n s(t))$  and  $I_R(t) = r(t)(I + k_n s(t))$ . The adaptive gain is obtained here as an asymmetric sigmoidal function of  $d_{\min}/L$ , i.e., of the minimum distance measured by the full sensor array (cf. Fig. 1), normalized by the mechanism's length. The combination of reactive centering with amplitude shaping is demonstrated for the seven-link undulatory mechanism in Fig. 4.

### 3.3. Formation control of undulatory swarms

One of the approaches, proposed to address the problem of collective exploration by multiple vehicles, involves the definition of swarm behavior primitives, like collective movement along parallel or circular trajectories. Typically, this requires that each vehicle has information regarding the range from and relative orientation to the other swarm members [17,29]; this information can be obtained in a distributed manner by sensors on-board each vehicle (e.g., a combination of vision and laser sensors). By appropriate switching between behavior primitives, the swarm can collectively track piecewise-linear trajectories of a moving target or reference agent.

A variation of the ‘‘circling’’ control law, proposed in [17] for multiple unit-speed vehicles, is employed here, where a circling formation emerges by steering controls alone. Such circling behaviors are relevant to applications where multiple vehicles are required to stay near a reference agent, real or virtual. Adaptation to a swarm of  $n$  undulatory mechanisms, all controlled by identical locomotor CPGs, involves setting the tonic drive of the  $j$ th

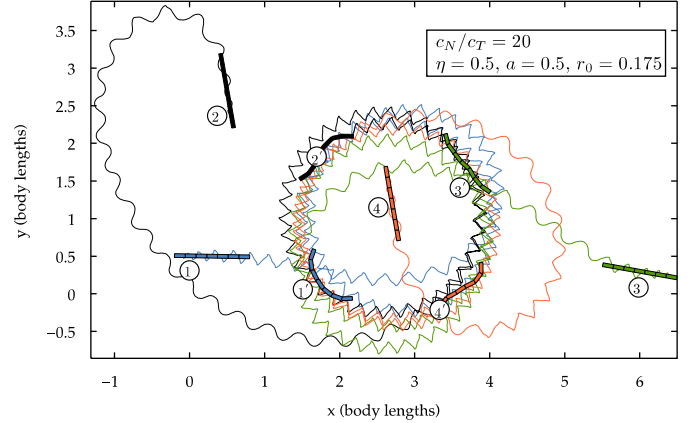


Fig. 5. Neural control of a swarming behavior, for eel-like locomotion: circular formation control for  $n = 4$  identical undulatory robots.

swarm member to

$$I_L^j(t) = I - g_j(t) \quad \text{and} \quad I_R^j(t) = I + g_j(t). \quad (6)$$

The sensor-modulated component  $g_j(t)$  above is obtained as

$$g_j = \frac{1}{n} \sum_{k \neq j} (-\eta \sin \varphi_j + f(\rho_{jk}) \cos \varphi_j), \quad (7)$$

where  $f(r) = a[1 - (r_0/r)^2]$  and  $\eta, a$  and  $r_0$  are all positive constants. Considering the  $(j, k)$ -th-pair of undulatory robots,  $\rho_{jk}$  denotes the distance between their head link centers, while  $\varphi_j$  and  $\varphi_k$  is the orientation of the head links with respect to the direction perpendicular to the baseline connecting the centers of the head links. To comply with the unit-speed assumption, the tonic input level is the same for all undulatory mechanisms in the swarm.

Indicative simulation results for an undulatory swarm under this formation control law, are shown in Fig. 5. The robots start at random initial positions (labeled 1–4) and, after a transient, they distribute themselves evenly on the periphery of a circle, which they trace (final positions are labeled 1'–4').

The motivation behind our application of this scheme to undulatory swarms stems from its simplicity, robustness and extensibility, as well as from its potential to be combined with reactive centering [32].

## 4. Conclusions

Several biomimetic neuromuscular control schemes, giving rise to closed-loop reactive behaviors for undulatory robots, have been presented and evaluated in simulation for various robot morphologies and types of interaction with the environment. These schemes, which include centering in corridor environments, and formation control for swarms of multiple undulatory robots, are based on distance sensors distributed on the body of the robot. Their data (unprocessed with respect to the effects of the undulatory dynamics) are used to modulate the tonic input

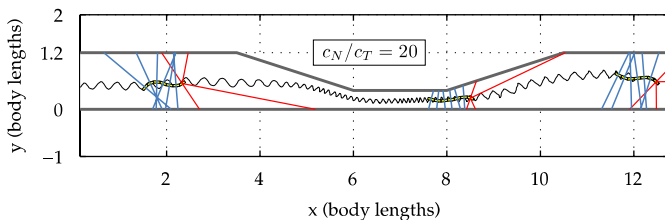


Fig. 4. Integrating reactive amplitude shaping with undulatory centering: tail link trajectory ( $I = 0.55$ ).

of the locomotor CPG, in order to reactively shape the propulsive undulatory wave. These neuromuscular control schemes are currently being extended to modes of locomotion involving active lateral parapodia-like appendages in the robot links (cf. motoneurons  $M_p$  in Fig. 2). Extensions of the developed control schemes to undulatory robots equipped with limited-range sensors are also being pursued.

In related work, several polychaete-like robotic prototypes have been used to demonstrate undulatory locomotion on sand and pebbles. Experiments performed with them, show good agreement with the predictions of the computational models used in the present paper [34,31]. This provides early evidence regarding the plausibility of the presented neuromuscular robot control schemes, which are expected to be tested experimentally with appropriate prototypes equipped with exteroceptive sensors.

### Acknowledgments

This research was supported in part by the European Commission through the IST projects BIOLOCH (IST-2001-34181) and GNOSYS (FP6-003835). D.P.T. thanks P.S. Krishnaprasad, E. Niebur and A. Ijspeert for insightful discussions. The authors thank A. Vlaikidis for assistance in early phases of this work, as well as the members of the BIOLOCH consortium for their input. Related papers and videos can be found at the Web site (<http://www.ics.forth.gr/~tsakiris>).

### References

- [1] Y. Aloimonos, D.P. Tsakiris, On the visual mathematics of tracking, *Image Vision Comput.* 9 (4) (1991) 21–30.
- [2] M.A. Arbib (Ed.), *The Handbook of Brain Theory and Neural Networks*, MIT Press, Cambridge, MA, 1995.
- [3] A.A. Argyros, D.P. Tsakiris, C. Groyer, Biomimetic centering behavior for mobile robots with panoramic sensors, *IEEE Robot. Automat. Mag.* 11 (4) (2004) 21–30.
- [4] J. Ayers, *Neurotechnology for Biomimetic Robots*, MIT Press, Cambridge, 2003.
- [5] A.M. Bloch, P.S. Krishnaprasad, J.E. Marsden, R.M. Murray, Nonholonomic mechanical systems with symmetry, *Arch. Ration. Mech. Anal.* 136 (1996) 21–99.
- [6] R.C. Brusca, G.J. Brusca, *Invertebrates*, Sinauer Associates, Sunderland, 1990.
- [7] J. Conradt, P. Varshavskaya, Distributed central pattern generator control for a serpentine robot, in: *Proceedings of the Joint International Conference on Artificial Neural Networks and Neural Information Processing (ICANN/ICONIP)*, Istanbul, Turkey, 2003.
- [8] J. Cortes, S. Martinez, J.P. Ostrowski, K.A. McIsaac, Optimal gaits for dynamic robotic locomotion, *Int. J. Robot. Res.* 20 (9) (2001) 707–728.
- [9] F.J. Eisenhart, T.W. Cacciatore, W.B. Kristian Jr., A central pattern generator underlies crawling in the medicinal leech, *J. Comput. Physiol. A* 186 (2000) 631–643.
- [10] Ö. Ekeberg, A combined neuronal and mechanical model of fish swimming, *Biol. Cybern.* 69 (5–6) (1993) 363–374.
- [11] J. Gray, *Annelids*, in: *Animal Locomotion*, Weidenfeld & Nicolson, London, 1968, pp. 377–410.
- [12] S. Grillner, The motor infrastructure: from ion channels to neuronal networks, *Nat. Rev.* 4 (2004) 573–586.
- [13] S. Hirose, *Biologically Inspired Robots: Snake-Like Locomotors and Manipulators*, Oxford University Press, New York, 1993.
- [14] A.J. Ijspeert, A connectionist central pattern generator for the aquatic and terrestrial gaits of a simulated salamander, *Biol. Cybern.* 85 (5) (2001) 331–348.
- [15] A.J. Ijspeert, M. Arbib, Visual tracking in simulated salamander locomotion, in: J.A. Meyer, A. Berthoz, D. Floreano, H. Roitblat, S.W. Wilson (Eds.), *Proceedings of the Sixth International Conference of The Society for Adaptive Behavior (SAB'00)*, MIT Press, Cambridge, MA, 2000, pp. 88–97.
- [16] A.J. Ijspeert, A. Crespi, J.M. Cabelguen, Simulation and robotics studies of salamander locomotion. Applying neurobiological principles to the control of locomotion in robots, *Neuroinformatics* 3 (3) (2005) 171–196.
- [17] E.W. Justh, P.S. Krishnaprasad, Equilibria and steering laws for planar formation, *Syst. Control Lett.* 52 (1) (2004) 25–38.
- [18] N. Kopell, Toward a theory of modelling central pattern generators, in: A.H. Cohen, S. Rossignol, S. Grillner (Eds.), *Neural Control of Rhythmic Movements in Vertebrates*, Wiley, New York, 1988.
- [19] N. Kopell, G.B. Ermentrout, Chains of oscillators in motor and sensory systems, in: M.A. Arbib (Ed.), *The Handbook of Brain Theory and Neural Networks*, MIT Press, Cambridge, MA, 2003, pp. 201–205.
- [20] P.S. Krishnaprasad, D.P. Tsakiris, Oscillations, SE(2)-snakes and motion control: a study of the roller racer, *Dynamical Syst.* 16 (4) (2001) 347–397.
- [21] J.V. Lawry, Mechanisms of locomotion in the polychaete *Harmothoe*, *Comp. Biochem. Physiol.* 37 (2) (1970) 167–179.
- [22] Z. Lu, S. Ma, B. Li, Y. Wang, Serpentine locomotion of a snake-like robot controlled by cyclic inhibitory CPG model, in: *Proceedings of the IEEE/RSJ International Conference on Intelligent Robots and Systems (IROS'05)*, Edmonton, Canada, 2005, pp. 96–101.
- [23] E. Marder, D. Bucher, Central pattern generators and the control of rhythmic movements, *Curr. Biol.* 11 (23) (2001) R986–R996.
- [24] J.D. Murray, *Mathematical Biology I*, third ed., Springer, New York, 2002.
- [25] R.M. Murray, Nonlinear control of mechanical systems: a Lagrangian perspective, *Annu. Rev. Control* 21 (1997) 31–42.
- [26] E. Niebur, P. Erdős, Modeling locomotion and its neural control in nematodes, *Commun. Theor. Biol.* 3 (2) (1993) 109–139.
- [27] G.N. Orlovsky, T.G. Deliagina, S. Grillner, *Neuronal Control of Locomotion: from Mollusc to Man*, Oxford University Press, Oxford, 1999.
- [28] R.H. Rand, A.H. Cohen, P.J. Holmes, Systems of coupled oscillators as models of central pattern generators, in: A.H. Cohen, S. Rossignol, S. Grillner (Eds.), *Neural Control of Rhythmic Movements in Vertebrates*, Wiley, New York, 1988.
- [29] R. Sepulchre, D.A. Paley, N. Leonard, Stabilization of planar collective motion: all-to-all communication, *IEEE Trans. Automat. Control*, to appear.
- [30] M. Sfakiotakis, D.P. Tsakiris, SIMUUN: a simulation environment for undulatory locomotion *Int. J. Model. and Simul.* 26 (4) (2006).
- [31] M. Sfakiotakis, D.P. Tsakiris, K. Karakasiliotis, Polychaete-like pedundulatory robotic locomotion. The 2007 IEEE International Conference on Robotics and Automation (ICRA'07), submitted for publication.
- [32] M. Sfakiotakis, D.P. Tsakiris, A. Vlaikidis, Biomimetic centering for undulatory robots, in: *Proceedings of the First IEEE/RAS-EMBS International Conference on Biomedical Robotics and Biomechanics (BIOROB'06)*, Pisa, Italy, 2006, pp. 744–749.
- [33] D.P. Tsakiris, A. Menciassi, M. Sfakiotakis, G. La Spina, P. Dario, Undulatory locomotion of polychaete annelids: mechanics, neural control and robotic prototypes, in: *The Annual Computational Neuroscience Meeting (CNS\*2004)*, Abstract #288, Baltimore, USA, 2004.
- [34] D.P. Tsakiris, M. Sfakiotakis, A. Menciassi, G. La Spina, P. Dario, Polychaete-like undulatory robotic locomotion, in: *Proceedings of the*

IEEE International Conference on Robotics and Automation (ICRA'05), Barcelona, Spain, 2005, pp. 3029–3034.



**Michael Sfakiotakis** received his bachelor's degree in Electrical Engineering from Aristotle University, Thessaloniki, Greece, in 1995; his M.Sc. degree in Communications, Control and DSP from Strathclyde University, Glasgow, U.K., in 1996; and his Ph.D. degree in Electrical Engineering from Heriot-Watt University, Edinburgh, U.K., in 2000. He is currently a Research Associate at the Institute of Computer Science of the Foundation for Research and Technology—

Hellas (FORTH) in Heraklion, Greece. His research interests are in the areas of biologically inspired robotics, locomotion control and systems modeling.



**Dimitris P. Tsakiris** is a Principal Researcher at the Institute of Computer Science of the Foundation for Research and Technology—Hellas (FORTH) and a visiting professor at the University of Crete in Heraklion, Greece. He received his B.S. degree from the Department of Electrical Engineering of the National Technical University of Athens, Greece, and his M.S. and Ph.D. degrees from the Department of Electrical Engineering of the University of Maryland at

College Park, U.S.A. Prior to his current position, he was a Marie Curie postdoctoral fellow in INRIA, Sophia-Antipolis, France. His research interests lie in the areas of biologically inspired robotics, nonlinear control, geometric mechanics and computational vision. He is a principal investigator and co-investigator of several European IST projects and research networks related to these research areas.